Diamond Detector Technology: Status and Perspectives

The RD42 Collaboration

M. Reichmann[*26], **A. Alexopoulos**[3], **M. Artuso**[22], **F. Bachmair**[26], **L. Bäni**[26],
M. Bartosik[3], **J. Beacham**[15], **H. Beck**[25], **V. Bellini**[2], **V. Belyaev**[14], **B. Bentele**[21],
E. Berdermann[7], **P. Bergonzo**[13], **A. Bes**[30], **J-M. Brom**[9], **M. Bruzzi**[5], **M. Cerv**[3],
G. Chiodini[29], **D. Chren**[20], **V. Cindro**[11], **G. Claus**[9], **J. Collot**[30], **J. Cumalat**[21],
A. Dabrowski[3], **R. D'Alessandro**[5], **D. Dauvergne**[30], **W. de Boer**[12], **C. Dorfer**[26],
M. Dünser[3], **V. Eremin**[8], **R. Eusebi**[27], **G. Forcolin**[24], **J. Forneris**[17], **H. Frais-Kölbl**[4],
L. Gallin-Martel[30], **M.L. Gallin-Martel**[30], **K.K. Gan**[15], **M. Gastal**[3], **C. Giroletti**[19],
M. Goffe[9], **J. Goldstein**[19], **A. Golubev**[10], **A. Gorišek**[11], **E. Grigoriev**[10],
J. Grosse-Knetter[25], **A. Grummer**[23], **B. Gui**[15], **M. Guthoff**[3], **I. Haughton**[24], **B. Hiti**[11],
D. Hits[26], **M. Hoeferkamp**[23], **T. Hofmann**[3], **J. Hosslet**[9], **J-Y. Hostachy**[30], **F. Hügging**[1],
C. Hutton[19], **H. Jansen**[3], **J. Janssen**[1], **H. Kagan**[15], **K. Kanxheri**[31], **G. Kasieczka**[26],
R. Kass[15], **F. Kassel**[12], **M. Kis**[7], **V. Konovalov**[15], **G. Kramberger**[11], **S. Kuleshov**[10],
A. Lacoste[30], **S. Lagomarsino**[5], **A. Lo Giudice**[17], **E. Lukosi**[28], **C. Maazouzi**[9],
I. Mandic[11], **C. Mathieu**[9], **M. Menichelli**[31], **M. Mikuž**[11], **A. Morozzi**[31], **J. Moss**[15],
R. Mountain[22], **S. Murphy**[24], **M. Muškinja**[11], **A. Oh**[24], **P. Oliviero**[17], **D. Passeri**[31],
H. Pernegger[3], **R. Perrino**[29], **F. Picollo**[17], **M. Pomorski**[13], **R. Potenza**[2], **A. Quadt**[25],
A. Re[17], **G. Riley**[28], **S. Roe**[3], **D.A. Sanz-Becerra**[26], **M. Scaringella**[5], **D. Schaefer**[3],
C.J. Schmidt[7], **S. Schnetzer**[16], **S. Sciortino**[5], **A. Scorzoni**[31], **S. Seidel**[23], **L. Servoli**[31],
S. Smith[15], **B. Sopko**[20], **V. Sopko**[20], **S. Spagnolo**[29], **S. Spanier**[28], **K. Stenson**[21],
R. Stone[16], **C. Sutera**[2], **B. Tannenwald**[15], **A. Taylor**[23], **M. Traeger**[7], **D. Tromson**[13],
W. Trischuk[18], **C. Tuve**[2], **L. Uplegger**[6], **J. Velthuis**[19], **N. Venturi**[18], **E. Vittone**[17],
S. Wagner[21], **R. Wallny**[26], **J.C. Wang**[22], **J. Weingarten**[25], **C. Weiss**[3], **T. Wengler**[3],
N. Wermes[1], **M. Yamouni**[30] and **M. Zavrtanik**[11]

[1]*Universität Bonn, Bonn, Germany*
[2]*INFN/University of Catania, Catania, Italy*
[3]*CERN, Geneva, Switzerland*
[4]*FWT, Wiener Neustadt, Austria*
[5]*INFN/University of Florence, Florence, Italy*
[6]*FNAL, Batavia, USA*
[7]*GSI, Darmstadt, Germany*
[8]*Ioffe Institute, St. Petersburg, Russia*
[9]*IPHC, Strasbourg, France*
[10]*ITEP, Moscow, Russia*
[11]*Jožef Stefan Institute, Ljubljana, Slovenia*
[12]*Universität Karlsruhe, Karlsruhe, Germany*

[13]*CEA-LIST Technologies Avancees, Saclay, France*
[14]*MEPHI Institute, Moscow, Russia*
[15]*The Ohio State University, Columbus, OH, USA*
[16]*Rutgers University, Piscataway, NJ, USA*
[17]*University of Torino, Torino, Italy*
[18]*University of Toronto, Toronto, ON, Canada*
[19]*University of Bristol, Bristol, UK*
[20]*Czech Technical University, Prague, Czech Republic*
[21]*University of Colorado, Boulder, CO, USA*
[22]*Syracuse University, Syracuse, NY, USA*
[23]*University of New Mexico, Albuquerque, NM, USA*
[24]*University of Manchester, Manchester, UK*
[25]*Universität Göttingen, Göttingen, Germany*
[26]*ETH Zürich, Zürich, Switzerland*
[27]*Texas A&M, College Park Station, TX, USA*
[28]*University of Tennessee, Knoxville, TN, USA*
[29]*INFN-Lecce, Lecce, Italy*
[30]*LPSC-Grenoble, Grenoble, France*
[31]*INFN-Perugia, Perugia, Italy*
[32]*California State University, Sacramento, CA, USA*
E-mail: `michael.reichmann@cern.ch`

The planned upgrade of the LHC to the High-Luminosity-LHC will push the luminosity limits above the original design values. Since the current detectors will not be able to cope with this environment ATLAS and CMS are doing research to find more radiation tolerant technologies for their innermost tracking layers. Chemical Vapour Deposition (CVD) diamond is an excellent candidate for this purpose. Detectors out of this material are already established in the highest irradiation regimes for the beam condition monitors at LHC. The RD42 collaboration is leading an effort to use CVD diamonds also as sensor material for the future tracking detectors. The signal behaviour of highly irradiated diamonds is presented as well as the recent study of the signal dependence on incident particle flux. There is also a recent development towards 3D detectors and especially 3D detectors with a pixel readout based on diamond sensors.

The European Physical Society Conference on High Energy Physics
5-12 July
Venice, Italy

---

*Speaker.

1. Introduction

The upgrade of the Large Hadron Collider (LHC) to the High-Luminosity-LHC (HL-LHC) from 2023 to 2025 [1] will push the luminosity limits even above the original design values of the LHC and will therefore hopefully give us more insights in the fundamental nature of the universe. In 2028 an instantaneous luminosity of $5 \times 10^{34}\,\mathrm{cm^{-2}\,s^{-1}}$ is expected. In this environment the innermost tracking layer at a distance of $\sim 30\,\mathrm{mm}$ to the interaction point (IP) is expected to be exposed to a total fluence of $2 \times 10^{16}\,\mathrm{n_{eq}/cm^2}$ by 2028 [2]. This fluence is equivalent to an integrated luminosity of $\sim 3000\,\mathrm{fb^{-1}}$, but since the current pixel detectors are designed to withstand $\sim 300\,\mathrm{fb^{-1}}$ the full detector would have to be replaced about every year. This led to research and development of new radiation tolerant detector designs and materials.

Its large displacement energy of $42\,\mathrm{eV/atom}$ and a high band gap of $5.5\,\mathrm{eV}$ make diamond an excellent candidate for such a radiation tolerant detector which is why the RD42 Collaboration is investigating single-crystal (sc) and poly-crystalline (p) Chemical Vapour Deposition (CVD) diamond as an alternative for precision tracking detectors for over two decades. In order to grow high quality detector grade diamonds, RD42 works together with industrial companies. All results in this paper were acquired with scCVD diamonds produced by Element Six Technologies [3] and pCVD diamonds produced by II-VI Incorporated [4]. The main difference between the two types of diamonds are their sizes of $\sim 0.25\,\mathrm{cm^2}$ for scCVD and up to 6 inch for pCVD and the smaller signal in pCVD [5]. In various studies it was shown that compared to corresponding silicon detectors, diamond is at minimum three times more radiation hard [6], has at least a two times faster charge collection [7] and its thermal conductivity is four times higher [8].

It is essential for all modern collider experiments to have an online monitoring of the beam conditions as close as possible to the beam [1]. Due to the high radiation in that regime presently all of the four main experiments at the LHC are using detectors with diamond sensors. ATLAS [9], ALICE [10], CMS [11] and LHCb [12] all make use of various Beam Condition Monitors (BCMs) and/or Beam Loss Monitors (BLMs) based on both CVD type diamonds for live background estimations and luminosity measurements.

Due to expected high particle flux and expected radiation dose for the HL-LHC it is very important to understand the behaviour of future detectors in this environment. The RD42 Collaboration has studied CVD diamond detectors with irradiation doses up to $2.2 \times 10^{16}\,\mathrm{p/cm^2}$. In order to build more radiation tolerant detectors, a new technology - 3D detectors [13] - in diamond is being investigated [14] . The 3D design of these detectors heavily reduces the drift distance of the created charge carriers without reducing the total number of the created electron-hole pairs. Since the particle flux of the HL-LHC will be in completely new regime, high rate studies are performed at Paul Scherrer Institut (PSI) with nearly minimum ionising particles (MIPs) and tunable particle fluxes from the order of $1\,\mathrm{kHz/cm^2}$ up to the order of $10\,\mathrm{MHz/cm^2}$.

2. CVD Diamond Detectors in the ATLAS Diamond Beam Monitor (DBM)

During the long shutdown in 2014 ATLAS installed one of the first diamond pixel detectors - the DBM - as an upgrade of the BCM. Its purpose is to measure an instantaneous (bunch-by-bunch) luminosity and the bunch-by-bunch position of the beam spot. With its eight telescopes of which

each has three detector planes it adds tracking capability to the existing precise time-of-flight (ToF) measurements of the eight pad detectors of the BCM. Using state-of-the-art pixel detectors based on the FE-I4B readout chip (ROC) [15] increases the segmentation and the spatial resolution of the beam monitor and due to its projective geometry pointing towards the interaction region it can distinguish particles coming from collisions and background [16]. The telescopes - six of which are built from pCVD diamonds and two from silicon as reference - are positioned symmetrically around the beam pipe on both sides of the IP and are shown in Figure 1. A total number of 45 diamonds with a thickness of $500\,\mu m$ were available for the project of which 18 were chosen for the detector.

(a) positioning and alignment (from [16])

(b) four mounted telescopes
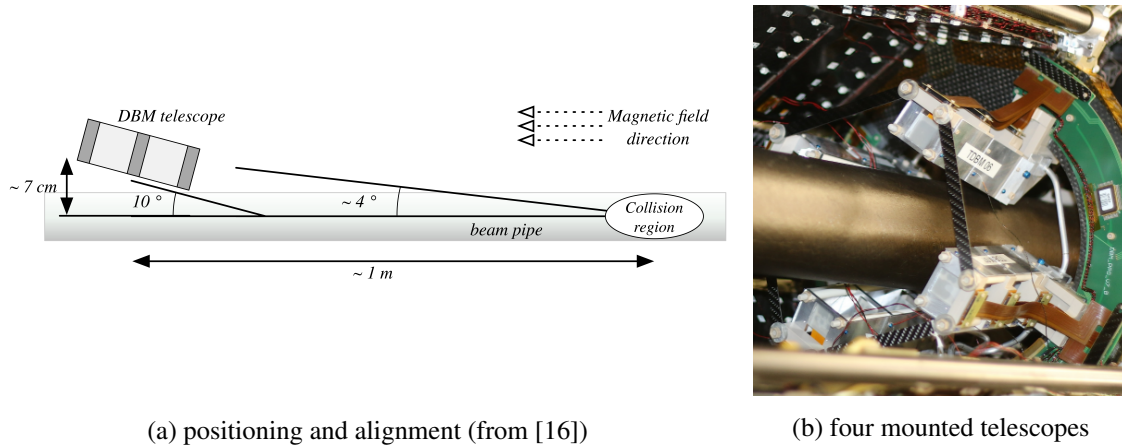
Figure 1: The positioning of DBM telescope around the beam pipe of the LHC

The first results already show a clear discrimination between collision and background events as demonstrated in Figure 2. During the shutdown of the LHC in the beginning of 2017 the modules were recommissioned and are now a part of the ATLAS data taking.
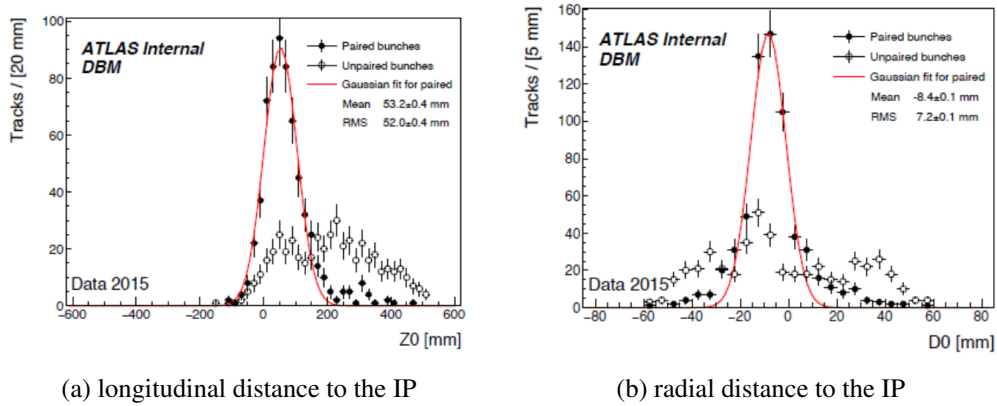

(a) longitudinal distance to the IP

(b) radial distance to the IP

Figure 2: Reconstruction of tracks from three modules using the initial alignment.

3. Radiation Tolerance

In order to probe the radiation tolerance of CVD diamond sensors several radiation studies

Particle	Energy	Relative κ
Proton	24 GeV	1.0
	800 MeV	1.79 ± 0.13
	70 MeV	2.4 ± 0.4
	25 MeV	4.5 ± 0.6
Neutron	∼1 MeV	4.5 ± 0.5
Pion	200 MeV	$2.5 - 3$

Table 1: Damage constants for various irradiations normalised to 24 GeV protons

have been performed varying the types and energies of damaging particles. The sensors were irradiated with protons of different energies (24 GeV, 800 MeV, 70 MeV, 25 MeV), ∼1 MeV reactor neutrons and 200 MeV pions up to a maximum dose of 2.2×10^{16} p/cm^2 which is equivalent to ∼500 Mrad.

(a) At CERN PS [17]   (b) At LANL [5]
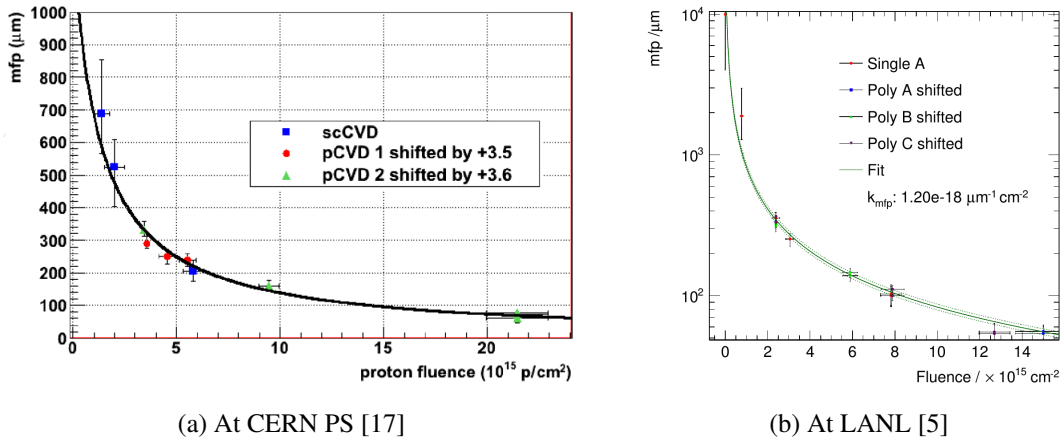
Figure 3: Irradiation results for proton energies of 24 GeV (a) and 800 MeV (b). The solid line in each plot is a fit using equation 3.1.

In order to build a detector out of a CVD diamond sensor a specific recipe is applied where the diamond is cleaned and metallised [18]. Depending on the geometry of the metallisation pattern, pad, strip and pixel detectors can be built. For the radiation studies, a strip pattern was chosen in order to correlate the pulse height with the position information.

The characterisation of the irradiated devices was performed at a Super Proton Synchrotron (SPS) beam line at CERN using charged hadrons with momenta of the order of 120 GeV/c. By using a customised beam telescope with a spatial resolution of ∼2 µm one obtains an unbiased hit prediction of the particle track in the diamond sensor.

The signal behaviour of irradiated material follows the simple damage equation

$$\frac{1}{\lambda} = \frac{1}{\lambda_0} + \kappa \phi \tag{3.1}$$

with the initial mean free path (MFP) λ_0, the damage constant κ and the fluence ϕ [5]. Since the measurable quantity is the charge collection distance (CCD) we make the assumption that the MFP of electrons and holes are the same which was studied in [5]. Due to that one can find a relation of the CCD to the MFP .

The results of two different types of irradiation are shown in Figure 3. As seen in the examples all of the tested samples follow the equation 3.1. Table 1 shows all the extracted damage constants.

4. High Rate Beam Tests

In addition to the radiation studies it is very important to understand the effect of the incident particle flux on the signal of CVD diamonds. In order to conduct such a study it is essential to be able to vary the particle flux over a large range. The πM1 beam line at the High Intensity Proton Accelerator (HIPA) at PSI [19] can provide beams with continuously tunable fluxes from the order of $1\,kHz/cm^2$ up to $10\,MHz/cm^2$ which have a spacing of 19.8 ns between each bunch. For these studies a π^+ beam with with a momentum of 260 MeV/c was chosen in order to reach the highest possible flux [20].

The diamond sensors were connected in a pad geometry and prepared as described in [21]. In order to resolve single waveforms at high particle rates the sensors were connected to a fast, low-noise amplifier with a rise time of approximately 5 ns. The resulting waveforms were then read out with a DRS4 Evaluation Board at a sampling frequency of 2 GHz. The final diamond pad detectors were measured in a beam telescope based on the CMS pixel ROCs PSI46v2 [22] which provides tracking with an inherent resolution of ∼70 μm at the position of the DUT. A better resolution can be achieved by applying a cut on the χ^2 distribution of the tracks. The telescope did also provide a trigger of which the area can be masked to increase the efficiency of the data taking. A scintillator was positioned at the end of the telescope to achieve a precise timing of 1 ns.

An overlay of 30 000 resulting waveforms is shown in Figure 4. The most frequent peak at ∼70 ns is caused by the actual particle which was triggered on. The region of 20 ns around this mean peak position is called signal region. All the other peaks are from particles of other bunches. Due to the good timing resolution the bunch spacing of the PSI beam can be clearly seen in the plot. The bunch just before the signal region is forbidden by the trigger logic and is used to extract the pedestal (base line) of the waveform. The pulse height value is then calculated by averaging the waveform in a 10 ns window around the maximum value in the signal region.
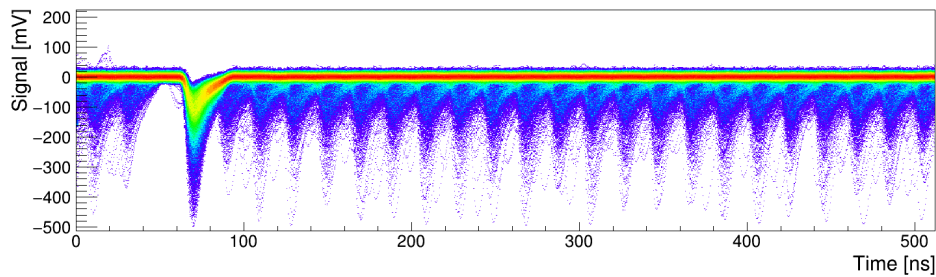

Figure 4: Overlay of 30000 waveforms

In order to exclude a dependence on the incident particle flux several rate scans with both polarities of the bias voltage and different irradiation doses were performed. The typical scan starts at the minimum flux, goes up to the maximum (up scan) and then goes down to the minimum again (down scan). In addition, random scan were done whereby systematic effects were excluded.

4

Figure 5 shows the final results for a pCVD diamond both non-irradiated and irradiated with reactor neutrons to 5×10^{14} n/cm^2 . An upper limit for a pulse height dependence on particle flux of less than 5 % was observed for a flux up to 20 MHz/cm^2. In addition it can also be seen this there is a slight difference between positive and negative bias which is due to the electronics. After the irradiation the pulse height decreases due to the radiation damage. There was no absolute calibration done yet which is required to relate the pulse height values before and after irradiation.
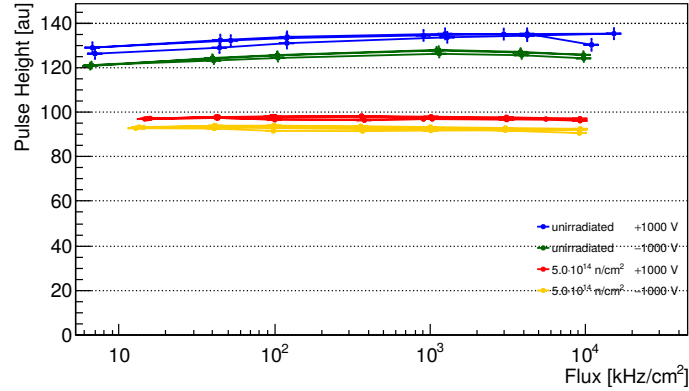

Figure 5: Pulse height versus incident particle flux for a pCVD diamond for irradiated and non-irradiated detectors

5. 3D Detectors

After large irradiation, all detector materials become trap limited with a MFP below 75 μm. The concept of a 3D detector is a possible way to reduce the drift distance below the this MFP. More details about the fabrication and the functionality can be found in [14], [13].

In 2015 the first detector was built out of a pCVD diamond sensor which had 3D readout with ganged readout columns as well as a strip metallisation on the same sensor. The thickness of sensor was ∼500 μm and the 3D cells had a size of 150 μm × 150 μm. At this time the column production efficiency was about 92 % [5]. The mean of the measured pulse height is 13 500 e which is much higher than 6900 e in the strip detector on the same diamond. The strip signal equates to a CCD of 192 μm whereas the charge in the 3D would have a CCD in a planar detector of 350 μm to 375 μm which effectively means that more than 75 % of the created charge was collected for the first time in a pCVD diamond. The corresponding pulse height distributions are shown in Figure 6. This detector was already a success by showing a working 3D diamond detector.
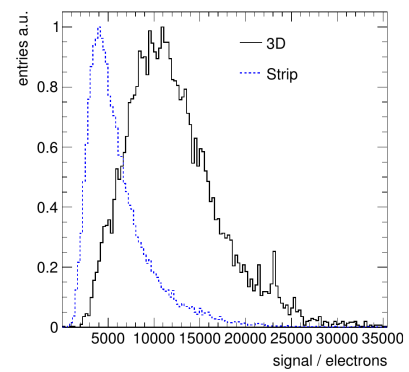

Figure 6: Pulse height of the 3D multi detector

In 2016 a full 3D detector was constructed with dramatic improvements. The number of cells was scaled up from 99 to 1188, the cell size was reduced to to 100 μm × 100 μm and the column

production efficiency was increased to 99 %. The analysis of this device is still in progress but the first results already show charge in the entire area of the detector and it has the largest charge collection in pCVD with over 85 % in a contiguous region.

Finally at the end of 2016 the first pCVD 3D sensor with pixel readout which was metallised and then bump bonded to a CMS pixel ROC PSI46digV2.1respin [22]. The chip was then tuned to a global pixel threshold of 1500 e. The preliminary beam test results show an efficiency of 98.5 %. This value is close to the efficiency of a silicon pixel of 99.3 % which was tested in parallel. Compared to the silicon the 3D pixel detector has a relative efficiency of 99.2 %. The loss of 0.8 % is believed to originate from the low field regions between the electrodes.

6. Conclusion

By now the technology of diamond detectors is well established in high energy physics. Many of the experiments are already using BCMs or BLMs based on CVD diamonds. As one of the first pixel projects the ATLAS DBM was recommissioned for the 13 TeV collisions and started taking data.

The diamond material was proven to be very radiation tolerant and the signal behaviour after the irradiation with various particle species and energies is well understood for both scCVD and pCVD diamonds. In extensive studies it was found that pCVD diamond detectors work reliably and show no signal dependence up to an incident particle flux of 20 MHz/cm^2. This was also shown for irradiated detectors up to fluence of 5×10^{14} n_{eq}/cm^2.

There is also great progress in the development of more radiation tolerant devices. The working principle of both 3D strip and pixel detectors was proven with great success down to cell sizes of 100 μm × 100 μm. For the first time more than 80 % of the created charge in the material was read out. The efficiency of the column drilling process is now above 99 % and the relative efficiency of the 3D pixel detectors is 99.3 % compared to a silicon detector.

References

[1] G. Apollinari, I. Béjar Alonso, O. Brüning, M. Lamont, and L. Rossi, *High-Luminosity Large Hadron Collider (HL-LHC): Preliminary Design Report*. CERN Yellow Reports: Monographs, Geneva: CERN, 2015.

[2] G. Auzinger, "Upgrade of the CMS Tracker for the High Luminosity LHC," Tech. Rep. CMS-CR-2016-268, CERN, Geneva, Oct 2016.

[3] "Element Six Technologies." `https://e6cvd.com`, 2017.

[4] "II-VI Incorporated." `http://www.ii-vi.com`, 2017.

[5] F. Bachmair, *CVD Diamond Sensors In Detectors For High Energy Physics*. PhD thesis, Zurich, ETH, 2016.

[6] W. de Boer, J. Bol, A. Furgeri, S. Müller, C. Sander, E. Berdermann, M. Pomorski, and M. Huhtinen, "Radiation hardness of diamond and silicon sensors compared," *physica status solidi (a)*, vol. 204, no. 9, pp. 3004–3010, 2007.

[7] H. Pernegger, V. Eremin, H. Frais-Kölbl, E. Griesmayer, H. Kagan, S. Roe, S. Schnetzer, R. Stone, W. Trischuk, D. Twitchen, P. Weilhammer, and A. Whitehead, "Charge-carrier properties in synthetic single-crystal diamond measured with the transient-current technique," *J. Appl. Phys.*, vol. 97, no. 7, pp. 73704–1–9, 2005.

[8] S. Zhao, *Characterization of the electrical properties of polycrystalline diamond films*. PhD thesis, The Ohio State University, 1994.

[9] A. Goriŝek, V. Cindro, I. Dolenc, H. Frais-Kölbl, E. Griesmayer, H. Kagan, S. Korpar, G. Kramberger, I. Mandi, M. Meyer, M. Miku, H. Pernegger, S. Smith, W. Trischuk, P. Weilhammer, and M. Zavrtanik, "ATLAS diamond Beam Condition Monitor," *Nuclear Instruments and Methods in Physics Research Section A: Accelerators, Spectrometers, Detectors and Associated Equipment*, vol. 572, no. 1, pp. 67 – 69, 2007. Frontier Detectors for Frontier Physics.

[10] M. Hempel, W. Lohmann, and S. Rüdiger, "Application of Diamond Based Beam Loss Monitors at LHC," May 2013. Presented 26 Nov 2012.

[11] E. Bartz, J. Doroshenko, V. Halyo, B. Harrop, D. Hits, D. Marlow, L. Perera, S. Schnetzer, and R. Stone, "The PLT: A Luminosity Monitor for CMS Based on Single-Crystal Diamond Pixel Sensors," *Nuclear Physics B - Proceedings Supplements*, vol. 197, no. 1, pp. 171 – 174, 2009. 11th Topical Seminar on Innovative Particle and Radiation Detectors (IPRD08).

[12] M. Domke, C. Ilgner, S. Kostner, M. Lieng, M. Nedos, J. Sauerbrey, S. Schleich, B. Spaan, and K. Warda, "Commissioning of the beam conditions monitor of the LHCb experiment at CERN," in *2008 IEEE Nuclear Science Symposium Conference Record*, pp. 3306–3307, Oct 2008.

[13] S. Parker, C. Kenney, and J. Segal, "3D - A proposed new architecture for solid-state radiation detectors," *Nuclear Instruments and Methods in Physics Research Section A: Accelerators, Spectrometers, Detectors and Associated Equipment*, vol. 395, no. 3, pp. 328 – 343, 1997. Proceedings of the Third International Workshop on Semiconductor Pixel Detectors for Particles and X-rays.

[14] F. Bachmair, L. Bäni, P. Bergonzo, B. Caylar, G. Forcolin, I. Haughton, D. Hits, H. Kagan, R. Kass, L. Li, A. Oh, S. Phan, M. Pomorski, D. Smith, V. Tyzhnevyi, R. Wallny, and D. Whitehead, "A 3D diamond detector for particle tracking," *Nuclear Instruments and Methods in Physics Research Section A: Accelerators, Spectrometers, Detectors and Associated Equipment*, vol. 786, pp. 97 – 104, 2015.

[15] M. Backhaus *et al.*, "Characterization of the FE-I4B pixel readout chip production run for the ATLAS Insertable B-layer upgrade," *JINST*, vol. 8, p. C03013, Mar 2013.

[16] M. Cerv *et al.*, "The ATLAS diamond beam monitor," *Journal of Instrumentation*, vol. 9, p. C02026, 02 2014.

[17] J. Tsung and N. Wermes, "Diamond and Silicon Pixel Detectors in High Radiation Environments," 2012. Presented 2012.

[18] H. Kagan and W. Trischuk, "Radiation Sensors for High Energy Physics Experiments," in *CVD diamond for electronic devices and sensors* (R. Sussmann, ed.), ch. 9, pp. 207–227, Chichester: John Wiley & Sons, 2009.

[19] "High Intesity Proton Accelerator at PSI." `https://www.psi.ch/rf/hipa`, 2017.

[20] "Pion and electron fluxes in piM1." `http://aea.web.psi.ch/beam2lines/pim1c.html`, 2015.

[21] R. Wallny *et al.*, "Beam test results of the dependence of signal size on incident particle flux in diamond pixel and pad detectors," *JINST*, vol. 10, no. 07, p. C07009, 2015.

[22] A. Kornmayer, T. Müller, and U. Husemann, "Studies on the response behaviour of pixel detector prototypes at high collision rates for the CMS experiment," Nov 2015. Presented 04 Dec 2015.